Vortex nucleation in spin-torque nanocontact oscillators

T. Devolder,[1,a)] Joo-Von Kim,[1] M. Manfrini,[2,3] W. van Roy,[2] L. Lagae,[2,3] and C. Chappert[1]
[1]*Institut d'Electronique Fondamentale, UMR 8622, CNRS, Orsay 91405, France and Univ. Paris-Sud, Orsay 91405, France*
[2]*IMEC, Kapeldreef 75, B-3001 Leuven, Belgium*
[3]*Laboratorium voor Vaste-Stoffysica en Magnetisme, K. U. Leuven, Celestijnenlaan 200 D, B-3001 Leuven, Belgium*

(Received 29 April 2010; accepted 23 July 2010; published online 20 August 2010)

We present an experimental study of the nucleation rate associated with current-driven vortex oscillations in magnetic nanocontacts. We find that the nucleation and subsequent steady-state oscillation of a vortex can be initiated using current pulses as short as a few nanoseconds, yielding instant on oscillator capability. The nucleation rate is governed by an Arrhenius law, with an exponential dependence on the applied current magnitude. The mechanism for the vortex nucleation is discussed and compared to analytical estimates assuming the transient presence of a vortex-antivortex pair. © *2010 American Institute of Physics*. [doi:10.1063/1.3478843]

The dynamics of magnetic vortices has drawn considerable attention over the past decade because of the rich physical phenomena associated with such nonlinear objects and potential applications in information storage and processing. A system that facilitates the study of magnetic vortex dynamics in extended media, as opposed to the confined submicronic structures typically used, is the magnetic nanocontact. In this system, large current densities flow through a magnetoresistive multilayer structure via a nanoscale metallic contact, which leads to large spin-torque effects and oersted-ampere fields that drive vortex motion. Furthermore, a steady-state oscillation that comprises an orbital motion of the vortex around the nanocontact can be made possible.[1–5] As a result of this dynamics, a stable oscillation in the nanocontact resistance (through the giant magnetoresistance effect) is generated in the 100–500 MHz range, which allows the possibility of exploiting such systems as compact microwave sources,[6] which can operate at zero applied field,[3] possessing multioctave frequency coverage with an exceptional agility.[7]

One important aspect of such vortex oscillator dynamics concerns the "boot time," i.e., the delay between the application of an external control parameter (such as the current) and the start of steady-state oscillations. This point is particularly relevant for mobile applications for which energy management is crucial. From a fundamental perspective, it is interesting and important to understand the physical process by which vortex oscillations can be initiated from a uniform magnetic state in an extended film, given that the topology of the initial and final states are so different.

In this article, we present an experimental study of the nucleation rate of vortex oscillations in a magnetic nanocontact system. The study is conducted under zero applied fields, whereby the initial state is free of any vortex structure. The nucleation processes are initiated under pulsed currents and oscillations, if they occur, are subsequently registered in the frequency domain. The experimental results, combined with a simple analytical theory, suggest that the nucleation involves the creation of a vortex-antivortex pair, followed by the expulsion of the antivortex from the system.

The nanocontacts we studied are fabricated on spin-valves of composition $IrMn(6\ nm)/Co_{90}Fe_{10}(4.5\ nm)/Cu(3.5\ nm)/Co_{90}Fe_{10}(1.5\ nm)/Ni_{80}Fe_{20}(2\ nm)$, with a nominal contact diameter $2r_n=100$ nm. Note the importance of the oersted-ampere field in this geometry; For a current of 50 mA, the field at the contact edge reaches 0.2 T, which is much stronger than the intrinsic magnetocrystalline anisotropy field and comparable to demagnetizing fields. We write $d=3.5$ nm the free layer thickness. The phase noise, the linear tunability of 7.4 MHz/mA,[3] and the agility of a generic oscillator have been studied elsewhere.[7] The free layer has a magnetization of $\mu_0 M_s=1.56\pm0.05$ T and a Gilbert damping of $\alpha=0.013\pm0.002$.[8] We write $Ad=0.42$ eV for the thickness-integrated exchange stiffness of the free layer, which is calculated assuming bulk properties for Py, Co, and Fe.[9,10] Our devices have resistances of typically $R_P=9\ \Omega$ (including the series electrodes of 7.3 Ω) and a magnetoresistance of $\Delta R=25$ mΩ. The total resistance increases linearly with the temperature at 7.5 mΩ/K between 4 and 450 K. For the representative device studied in detail here, vortex nucleation with 52 mA is typically associated with a delay of 100 ms. Nanocontacts with nominal radii of 40, 50, 60, 80, and 100 nm generally also show vortex oscillations. Fluctuations during fabrication lead to some scattering in the effective nanocontact radii. However the dc nucleation currents were found to be inversely correlated with the device resistance, indicating a current-density based nucleation threshold.

The following procedure, which is presented schematically in Fig. 1, was followed to study the vortex nucleation by pulsed currents. First, we apply no current, which in zero field is known[3] to yield a vortex-free magnetic configuration in the region of interest in the vicinity of the nanocontact. A dc current of 14 mA is then applied at which a vortex-free reference voltage spectrum is recorded [Fig. 1(c)]. Note that for currents above 10 mA, the absence (respectively, the presence) of vortex could be certified by the value of the resistance and systematically correlated with an absence (respectively, the presence) of well defined spectral lines in the voltage noise spectrum.[3] The dc current is then increased into the range of $I_{bias}=44$ to 51.9 mA. After a few milliseconds,

a)Electronic mail: thibaut.devolder@u-psud.fr.

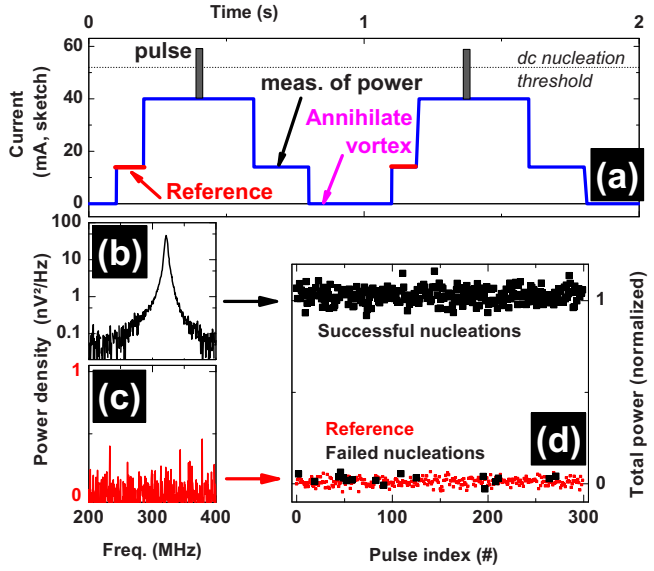

FIG. 1. (Color online) (a) Procedure used to measure the vortex nucleation probability. (b) Voltage noise power density for 14 mA when a vortex is present. (c) Idem when there is no vortex (reference curve, taken at the reference step of panel (a) before the nucleation attempt). (d) Total noise power before (small symbols) and after each current pulse (large squares).

we measure a maximum increase in the dc resistance of 0.44 Ω, indicating a device temperature bounded by 353 and approximately 500 K. Indeed if the electrodes and the nanocontact were isothermal, the resistance could be translated into a uniform temperature of 353 K. However since the electrodes are in contact to 300 K thermostats, there is a temperature gradient to the nanocontact. If all the resistance rise was due to a temperature rise of the sole nanocontact, this would mean a heating up to 500 K, probably not that far from the Curie temperature which is 853 K for bulk permalloy. After this thermalization time, an rf router is then latched to connect the device to a voltage pulse generator tuned to deliver a fixed $I_{\text{pulse}}=10.0$ mA, with a duration τ_{pulse} that varies from 0.1 to 10 ns. The rf router then brings the configuration back to a voltage spectrum measurement to discriminate between a nucleation with a clear microwave signature [Fig. 1(b)] and a featureless spectrum indicating no nucleation. The procedure is then repeated 300 times for each I_{bias} and τ_{pulse} to obtain the nucleation probabilities as a function of the total current, $I_{\text{total}}=I_{\text{bias}}+I_{\text{pulse}}$.

For a given current magnitude, the nucleation probability exhibits two clear regimes as the pulse duration is increased (see Fig. 2). A rapid increase in the cumulative nucleation probability is first observed for pulses up to t_{delay}

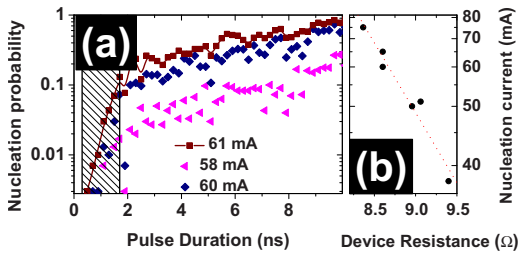

FIG. 2. (Color online) (a) Nucleation probability p vs pulse duration for several values of total applied current. The first 1.7 ns have been hatched. (b) Quasistatic nucleation current (reciprocal scale) vs device resistance at an applied temperature of 300 K.

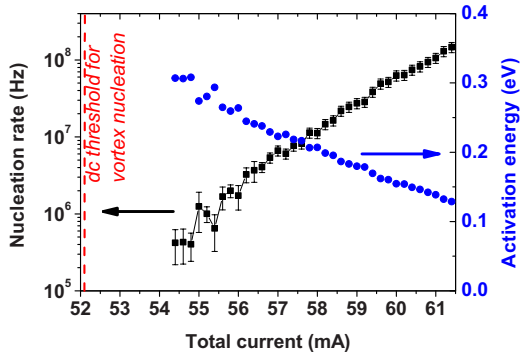

FIG. 3. (Color online) Left axis: Vortex nucleation rate Γ. Right axis: Deduced activation energy as a function of total current I_{total}, assuming a constant rate prefactor of 10 GHz and a device temperature of 353 K.

$\equiv 1.7\pm0.2$ ns, reaching a level of $p=p_{\text{delay}}$ that is well below 1. Since this delay is independent of the current and is of the same order as the micromagnetic relaxation time $2/(\alpha\gamma_0 M_S)=0.6$ ns, we infer that t_{delay} is related to the time needed to reach an equilibrium micromagnetic configuration. After this delay, the nucleation probability p gradually rises to 1 at a slower rate. This subsequent behavior is consistent with a constant nucleation rate Γ, which, after renormalizing by p_{delay} and t_{delay}, can be expressed in the relationship

$$\ln\left(\frac{1-p}{1-p_{\text{delay}}}\right)=-\Gamma(t-t_{\text{delay}}). \tag{1}$$

Based on existing results on thermally activated nucleation and reversal involving soliton–antisoliton pairs,[11] we can expect the nucleation rate to be governed by an Arrhenius law,

$$\Gamma=\Gamma_0 e^{-E_a/k_B T}, \tag{2}$$

where E_a is the activation energy and Γ_0 is a rate prefactor that is determined by the dynamics of crossing the activation barrier and the activation entropy. The nucleation frequency as a function of total applied current is presented in Fig. 3, where a quasiexponential current dependence is observed. If we assume current-independent rate pre-factor (10 GHz) and temperature, we find an activation energy that varies linearly with current. The activation energy extrapolates to zero for the deterministic nucleation current $I_{\text{nucl}}=66.3$ mA. The slope is $\partial E_a/\partial I=-3.2\times10^{-18}$ J/A, yielding a zero-current intercept $E_a=3.8\pm0.2$ $Ad=1.56$ eV.

Before proceeding further, we give some heuristic arguments for the most likely scenarios for vortex nucleation. It is assumed the free layer magnetization is uniform before the current pulse (and consequently the large oersted-ampere fields). To reach an orbiting vortex as a final state from this initial uniform state, some physical process that does not conserve topological charge needs to take place. Now, from a topological perspective, the uniform state possesses the same Skyrmion ($q=0$) and winding number ($n=0$) as a vortex-antivortex pair ($n=1$ for a vortex, $n=-1$ for an antivortex) with the same out-of-plane magnetization (polarization) p,[12] so it is possible to continuously deform the magnetization configuration to pass from one state to the other. In the absence of damping, such a vortex-antivortex pair is known to exhibit linear motion in the direction perpendicular to the pair axis. On the other hand a pair with opposite polarizations, while still retaining the same total winding number (and therefore ensuring a uniform magnetic configuration

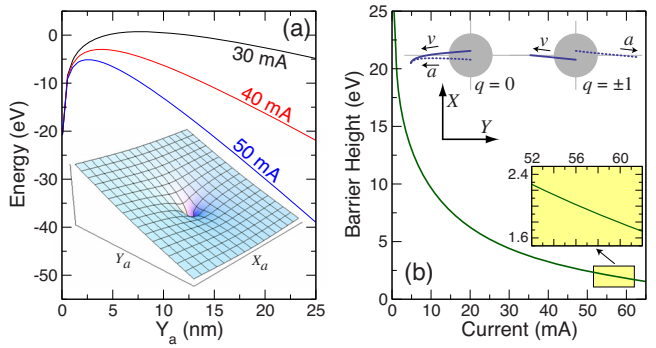

FIG. 4. (Color online) (a) Energy profile of a vortex-antivortex pair as a function of antivortex distance from contact center (X_a=0). Inset: Schematic profile of energy surface. (b) Energy barrier as a function of current, with a zoom on the experimental range as an inset (yellow). Top inset: Transient trajectories of vortex pairs with different Skyrmion numbers q, with the contact shown in gray. In both panels the calculations use the room temperature magnetic properties.

far from the pair), possesses a nonzero Skyrmion number ($q=\pm 1$) and therefore belongs to a different topological class. Such a pair exhibits rotational motion[13] and requires more energetic processes, related to Skyrmion decay or Bloch-point injection.[12,14] For both cases one might assume that the antivortex is eventually expelled from the system by the oersted-ampere field, leaving only the vortex behind.

To test the key aspects of this proposal, we have constructed a simple analytical and numerical theory that allows vortex pair energetics and dynamics to be studied easily. The approach is based on a rigid-vortex model in which a magnetic configuration for the vortex-antivortex pair is assumed and its dynamics is determined by a Thiele equation.[2] The model presupposes the existence of a vortex-antivortex pair and so only the transient pair dynamics can be followed in order to estimate whether antivortex expulsion is likely; processes involving pair creation and annihilation are beyond the scope of this treatment.

A likely activation barrier involves the competition between the exchange energy, which leads to an attractive interaction between the vortex and antivortex, and the Zeeman energy due to the oersted-ampere field, which favors separating the pair; to lowest order in the displacement variables $\vec{R}_{v,a} \equiv (X_{v,a}, Y_{v,a})$, which describe the position of the vortex (v) and antivortex (a) in the film plane, the total energy reads

$$E = 4\pi A d \ln\frac{\|\vec{R}_v - \vec{R}_a\|}{r_c} + \mu_0 M_s H_{\mathrm{Oe}}(\pi d r_n)\ln\frac{L}{r_n}(Y_v - Y_a), \tag{3}$$

where r_c is the core radius, $H_{\mathrm{Oe}}=I/(2\pi r_n)$ is the oersted-ampere field at the contact edge, and L is the system size. The winding numbers have been chosen to give a uniform magnetization along the positive x axis far from the pair. By assuming that the pair separation remains symmetric with respect to the contact ($\vec{R}_v=-\vec{R}_a$), we find an activation barrier of the form shown in Fig. 4(a). As the current increases, the Zeeman energy progressively favors the separation of the vortex-antivortex pair. The energy barrier is obtained as the difference between the energy at the peak and the energy at a one atomic spacing between the core centers [Fig. 4(b)]. Note that for currents in the range of interest, the energy barrier always corresponds to vortex-antivortex separations of the order of a few nanometers, for which the approximation $\vec{R}_v=-\vec{R}_a$ does not impact the calculation result.

While this barrier is a nonlinear function of the current, an approximate linear dependence is seen in the range of currents relevant to the experiment. Two additional points are worth noticing: the model predicts the correct order of magnitude for the deterministic nucleation current at which the activation energy changes sign. It however overestimates the activation energy by a factor of 5 to 10, depending on the assumptions made for the device temperature. Note that the two terms in the activation energy are proportional to M_s and A [see Eq. (3)]. This is another indication that the magnetization and the exchange stiffness are much reduced during the current pulse, which is consistent with a substantial temperature rise during the nucleation process. Such a high temperature is likely to ease the injection of the Bloch point needed to get opposite core polarizations within the vortex-antivortex pair.

Finally, we emphasize that while this energy surface leads to the expulsion of the vortex pair from the contact, the ensuing transient dynamics depend crucially on the Skyrmion number. For parallel core polarizations (q=0) the underlying linear motion eventually leads to pair annihilation as a result of damping, a feature that is independent of the nucleation site. In contrast a pair with opposite $p(q=\pm 1)$, which undergoes rotational motion, is expelled from the contact in opposite directions [top inset of Fig. 4(b)]. As the antivortex is expelled at a greater velocity than the vortex, we conjecture that the antivortex reaches the system edge before the vortex, at which it is expelled, and subsequently the vortex becomes attracted to the conic potential[2] of the oersted-ampere field.

This work has been supported by the Triangle de la Physique contract 2007-051T. M.M. is supported by the European Community under the Sixth FP for the Marie Curie RTN SPINSWITCH, Contract No. MRTN-CT-2006-027.

[1] M. R. Pufall, W. H. Rippard, M. L. Schneider, and S. E. Russek, Phys. Rev. B **75**, 140404 (2007).
[2] Q. Mistral, M. van Kampen, G. Hrkac, J.-V. Kim, T. Devolder, P. Crozat, C. Chappert, L. Lagae, and T. Schrefl, Phys. Rev. Lett. **100**, 257201 (2008).
[3] T. Devolder, J.-V. Kim, P. Crozat, C. Chappert, M. Manfrini, M. van Kampen, W. Van Roy, L. Lagae, G. Hrkac, and T. Schrefl, Appl. Phys. Lett. **95**, 012507 (2009).
[4] A. Ruotolo, V. Cros, B. Georges, A. Dussaux, J. Grollier, C. Deranlot, R. Guillemet, K. Bouze-houane, S. Fusil, and A. Fert, Nat. Nanotechnol. **4**, 528 (2009).
[5] D. V. Berkov and N. L. Gorn, Phys. Rev. B **80**, 064409 (2009).
[6] M. W. Keller, A. B. Kos, T. J. Silva, W. H. Rippard, and M. R. Pufall, Appl. Phys. Lett. **94**, 193105 (2009).
[7] M. Manfrini, T. Devolder, J.-V. Kim, P. Crozat, N. Zerounian, C. Chappert, W. Van Roy, L. La-gae, G. Hrkac, and T. Schrefl, Appl. Phys. Lett. **95**, 192507 (2009).
[8] T. Devolder, J.-V. Kim, M. Manfrini, G. Hrkac, P. Crozat, L. Lagae, T. Schrefl, and C. Chappert, Proc. SPIE **7398**, 739808 (2009).
[9] R. Hertel, S. Gliga, M. Fähnle, and C. M. Schneider, Phys. Rev. Lett. **98**, 117201 (2007).
[10] C. Bilzer, T. Devolder, J.-V. Kim, G. Counil, C. Chappert, S. Cardoso, and P. P. Freitas, J. Appl. Phys. **100**, 053903 (2006).
[11] H.-B. Braun, Phys. Rev. Lett. **71**, 3557 (1993).
[12] O. A. Tretiakov and O. Tchernyshyov, Phys. Rev. B **75**, 012408 (2007).
[13] S. Komineas, Phys. Rev. Lett. **99**, 117202 (2007).
[14] R. Hertel and C. M. Schneider, Phys. Rev. Lett. **97**, 177202 (2006).